catalysts

MDPI

Article

The Distribution and Strength of Brönsted Acid Sites on the Multi-Aluminum Model of FER Zeolite: A Theoretical Study

Miao He, Jie Zhang *, Rui Liu, Xiuliang Sun and Biaohua Chen

State Key Laboratory of Chemical Resource Engineering, Beijing University of Chemical Technology, Beijing 100029, China; hemiaobuct@126.com (M.H.); liuruibuct@126.com (R.L.); sunxl@mail.buct.edu.cn (X.S.); chenbh@mail.buct.edu.cn (B.C.)

* Correspondence: zhangjie@mail.buct.edu.cn; Tel.: +86-10-644-12054

Academic Editor: José R. B. Gomes

Received: 22 November 2016; Accepted: 23 December 2016; Published: 1 January 2017

Abstract: One of the fundamental issues in catalysis is to identify the catalytic active site. Due to its prominent pore topology and acidity, ferrierite (FER) zeolite has attracted extensive interest in various catalytic reactions such as isomerization of butenes. However knowledge on the active Brönsted acid site is still absent. In the present study, we perform extensive density functional theory calculations to explore the distribution and strength of the Brönsted acid sites and their potential catalytic activity for the double-bond isomerization of 1-butene to 2-butene. We employ a two-layered ONIOM scheme (our Own *N*-layered Integrated molecular Orbital + molecular Mechanics) to describe the structure and energetic properties of FER zeolite. We find that the hydrogen bond could improve the stability of Brönsted acid sites effectively, and, as a result, Al4-O6-Si2 and Al4-O-$(SiO)_2$-Al4 are the most stable sites for 1-Al substitution and 2-Al substitution, respectively. We further find that the Brönsted acid strength tends to decrease with the increase of Al contents and increase when the distance between the Al atoms is increased in 2-Al substitution. Finally it is demonstrated that the strength of acid sites determines the catalytic activity for the double bond isomerization of 1-butene to 2-butene.

Keywords: density functional theory (DFT); FER zeolite; multi-Al substitution; acid site distribution; acid strength

1. Introduction

Silicon-rich zeolites have been proved efficient catalysts in the solid-catalyzed reactions such as isomerization, alkylation, and etherification [1–3]. The catalytically active species in zeolites balance the negative charge of AlO_4^- tetrahedra. Silicon-rich zeolites exhibit a high number of crystallographically distinguishable framework T sites, occupied by Si or Al atoms, resulting in a variability of the Al sitting in the framework [4,5]. Since the proton bind to the AlO_4^- tetrahedral, forming the Brönsted acid site, the position of Al in frameworks of zeolites controls the distribution of the Brönsted acid sites, which, in turn, affects the catalytic activity and selectivity. Ferrierite (FER) zeolite is a medium pore aluminosilicate material, including two-dimensional intersecting channels with 8-membered rings (4.8 Å × 3.5 Å) and 10-membered rings (5.4 Å × 4.2 Å) [6,7]. Due to its prominent pore structure and Brönsted acidity, it has been proved to be an efficient catalyst for butene isomerization [8,9]. Extensive experimental and theoretical studies have been performed to understand the underlying origin of the high reactivity of FER [8–11]. Although it is generally believed that the Brönsted acid site is the active site for the isomerization process and that the unique pore structure plays an important role in the reactivity, the properties of the catalyst, such as the acid strength, acid density, and the location of the acid sites and their effect on the reactivity are still unclear in the literature.

More specifically, temperature programmed desorption (TPD), solid-state nuclear magnetic resonance (SSNMR), fourier transform infrared spectroscopy (FTIR), and catalytic evaluation of Brönsted acidity are currently applied to obtain information about the distribution of Al atoms and the relative acidities of the zeolites [4,12–15]. The conditions of zeolite synthesis and Al concentration in the framework were the main factors determining the distribution of Al in zeolites. However the exact arrangement of Si and Al atoms in the framework cannot be detected and thus it is hard to characterize the physical/chemical properties during the catalytic processes [16]. In order to understand the nature of the zeolites, the density function theory (DFT) was applied to investigate the distribution of Al and the acid strength of Brönsted acid sites in zeolites. Zhou et al. [17] have studied the location and acid strength of different Al substitutions in MCM-22 and found that the most favorable sites were T1, T3, and T4; T2 was the least favorable site and the acidities of the Al1(O3H)Si4 and Al4(O3H)Si1 sites were stronger than those of the Al3(O1H)Si2 site. The nature of the acid sites in CHA zeolite were studied and the presence of additional Al substitutions in the zeolite framework were found to have a significant effect on the deprotonation energies and base adsorption energies of acid sites [18]. Particular attention was paid to the presence of Al-O-Si-O-Al and Al-OSiOSiO-Al sequences in ZSM-5; the presence of Al-O-(Si-O)$_n$-Al (n = 1 or 2) sequences could result in a charge of properties of the AlO_4^- tetrahedral [19]. Sazama et al. [20] have also discussed the distribution of Al in Al-rich BEA, via experimental and theoretical methods, and revealed that high Al content can lead to a high content of Al-OSiO-Al. In addition, Al-OSiOSiO-Al sequences and the strength of the Brönsted sites were changed a little. Furthermore, FER zeolite is also reported to exhibit high selectivity and stability for isomerization reactions, which has been attributed to its specific pore structure and mild acidity [21]. The effect of the pore structure on reactions has been studied in detailed [11,22], but the influence of the various local configurations on Brönsted acid sites has been mentioned rarely. Therefore it is necessary to study the distribution of different amount of Al atoms and the acid strength of Brönsted acid sites in FER zeolite. Although the experiment research on these issues was mentioned a little, several DFT calculations were also carried out to investigate the distribution of Al in FER zeolite [23,24]. However their cluster model was so extremely small that it could not represent the various types of Al/Si distributions, which are believed to be significant in determining the catalytic reactivity in butene isomerization. The effect of the relationship between acid strength and the stability of the Brönsted acid sites on the catalytic properties was discussed also a little.

In the present study, to systematically explore the distribution and the strength of Brönsted acid sites in FER zeolite, we built a very large, structural, 90T model, containing a complete 10-membered ring and a complete 8-membered ring, and studied the substitution energy and deprotonation energy by employing the ONIOM (B3LYP/6-31G (d, p): AM1) method. The distribution and strength of Brönsted acid sites in the n-Al ($n \geq 1$) model for FER were obtained. In particular, the influence of the distance between the double Al atoms in 2-Al model on the distribution and strength of Brönsted acid sites was discussed. To further investigate the catalytic properties of FER zeolite, the double-bond isomerization of 1-butene to 2-butene at various Brönsted acid sites was studied. Moreover we also revealed the corresponding relationship of the catalytic performance between the distribution and strength of Brönsted acid sites on zeolite. These theoretical results are contributed to guide the experiment methods for designing the appropriate catalyst for reaction and understand the properties of the catalyst.

2. Results and Discussions

2.1. 1-Al Substitution

We first consider one Al in the FER zeolite. The computational details about models are shown in Section 3. The relative substitution energies (S_E(Al/Si)) are listed in Table 1. It is found that the Al4-O6-Si2 site, which is formed from an Al atom occupied with the T4 site, is most the stable location for Brönsted acid in 1-Al model. The highest stability is attributed to the formation of intra-zeolite

hydrogen bonds in the plane of the 6-membered ring. This result is in accordance with our previous studies in 52T clusters, by the same method [25]. As is confirmed in Figure 1, the H atom in the hydroxyl group of Al4-O6-Si2 interacts with the adjacent three oxygen atoms, with the distances 2.19, 2.42, and 2.91 Å, respectively. We further find that the Al2-O6-Si4 site can also form similar hydrogen bonds in the plane of the 6-membered ring, of lengths 2.29, 2.37 and 2.93 Å, but these exhibit a slightly higher S_E(Al/Si) of 8.2 kcal/mol than those of the Al4-O6-Si2 site. This may be caused by the special position of the T2 site. The S_E(Al/Si) of the Al1-O2-Si2 site is 5.3 kcal/mol, which is the second-stable location for the formation of the Brönsted acid site. This special site is located at the 8-membered window of the FER cage and its hydroxyl is located at the intersection of the 10-membered and 8-membered rings. Thus the Al1-O2-Si2 site is less affected by the steric hindrance than the Al2-O6-Si4 site. The Al1-O2-Si2 site is more likely to be an active center for chemical reactions. The Al1-O4-Si1, Al3-O7-Si4, and Al4-O7-Si3 sites show relatively high values of S_E(Al/Si), suggesting that it is difficult to form the Brönsted acid sites at these sites. However, the value of S_E(Al/Si) has a big difference within the results reported by Benco et al. [26]. This different result may be caused by the simple Al/Si substitution without the bonding of H atoms, as reported. The locations of the proton, as it compensates for the charge of Al/Si substitution, can affect the acid properties [27,28]. Feng et al. [29] have discussed the proton siting in FER zeolite and showed that different locations of the proton could cause different substitution energies for the same Al substitution site. On the other hand, some divergences of the substitution energy for the same Al substitution site have also been observed when different calculation methods were compared with each other [25,29–31].

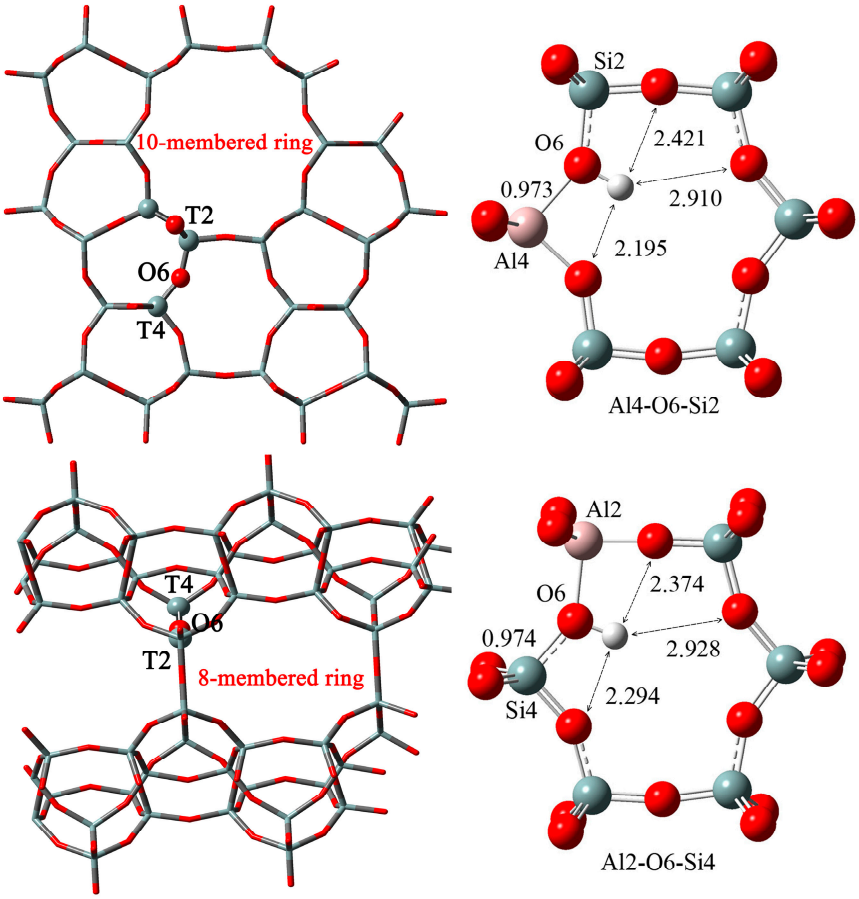

Figure 1. The location of T2-O6-T4 in framework and the structure parameters of hydrogen atoms in the hydroxyl group of Al4-O6-Si2 and Al2-O6-Si4 sites.

Table 1. S_E(Al/Si) and E_D of the different Brönsted acid sites of ferrierite (FER) zeolite.

Number	Brönsted Acid Sites	S_E(Al/Si) (kcal/mol)	E_D (kcal/mol)
0	Al1-O4-Si1	22.2	-
1	Al1-O1-Si3	8.3	5.8
2	Al1-O2-Si2	5.3	8.7
3	Al1-O3-Si1	7.0	7.1
4	Al2-O2-Si1	7.1	4.5
5	Al2-O5-Si2	8.7	1.9
6	Al2-O6-Si4	8.2	2.9
7	Al3-O1-Si1	7.2	3.7
8	Al3-O7-Si4	10.9	0.0
9	Al3-O8-Si3	7.2	3.7
10	Al4-O6-Si2	0.0	12.0
11	Al4-O7-Si3	11.4	-

We further consider the strengths of the Brönsted acidity at different sites. The relative deprotonation energy (E_D) is listed in Table 1. Due to its having the highest substitution energy, Al1-O4-Si1 hardly treated as a stable Brönsted acid site. If T4 is substituted by Al, the acidic proton should be located at Al4-O6-Si2 instead of Al4-O7-Si3 since the substitution energy difference is 11.4 kcal/mol. Therefore Al1-O4-Si1 and Al4-O7-Si3 were not studied further. Without surprise, the most stable site, Al4-O6-Si2, exhibited the weakest acidity with the highest E_D. Again this is attributed to the strong hydrogen-bond interaction between the proton and the adjacent lattice oxygen atoms, leading to difficulty in ionizing the acidic protons. In contrast, the Al3-O7-Si4 site, which has a relatively high S_E, exhibited the strongest acidity among all the 1-Al substitution sites. These results suggest that there is a balance between the stability and the Brönsted acidic strength. Although the Al2-O6-Si4 and Al4-O6-Si2 sites are located in the same 6-membered ring, the acid strength of the Al2-O6-Si4 site is much higher than that of the other one. The E_D of Brönsted acid sites such as Al2-O5-Si2, Al2-O6-Si4, and Al2-O2-Si1 are relatively low and these sites were concentrated in the region of the 8-membered ring, indicating that the Brönsted acid sites around the 8-membered ring have strong acidity. This also confirmed that the 8-membered ring has an important effect on the acid strength of Brönsted acid sites. However the stability of the Brönsted acid sites around the 8-membered ring has no obvious regularity, indicating that a large model containing a complete 8-memebered ring was taken into account in the effect of steric hindrance, compared with our previous studies [25].

2.2. n-Al Substitution (n ≥ 2)

After considering 1-Al substitutionin FER zeolite, we now first come to consider the distribution of Brönsted acid sites for 2-Al substitution. Here the most stable configuration in 1-Al substitution, Al4-O6-Si2, is kept as one of the two Brönsted acid sites. The other one is assumed to be either the Al1-O2-Si2 site or the Al4-O6-Si2 site because of their relatively high stability in 1-Alsubstitution. We especially consider the 1~3 SiO group between the two Al atoms, as is shown in Figure 2. Note that the Al-O-$(SiO)_2$-Al site has two different configurations; one has two Brönsted acid sites sharing the same 6-membered ring (Figure 2d), the other has two Brönsted acid sites in different rings (Figure 2a,b,c).

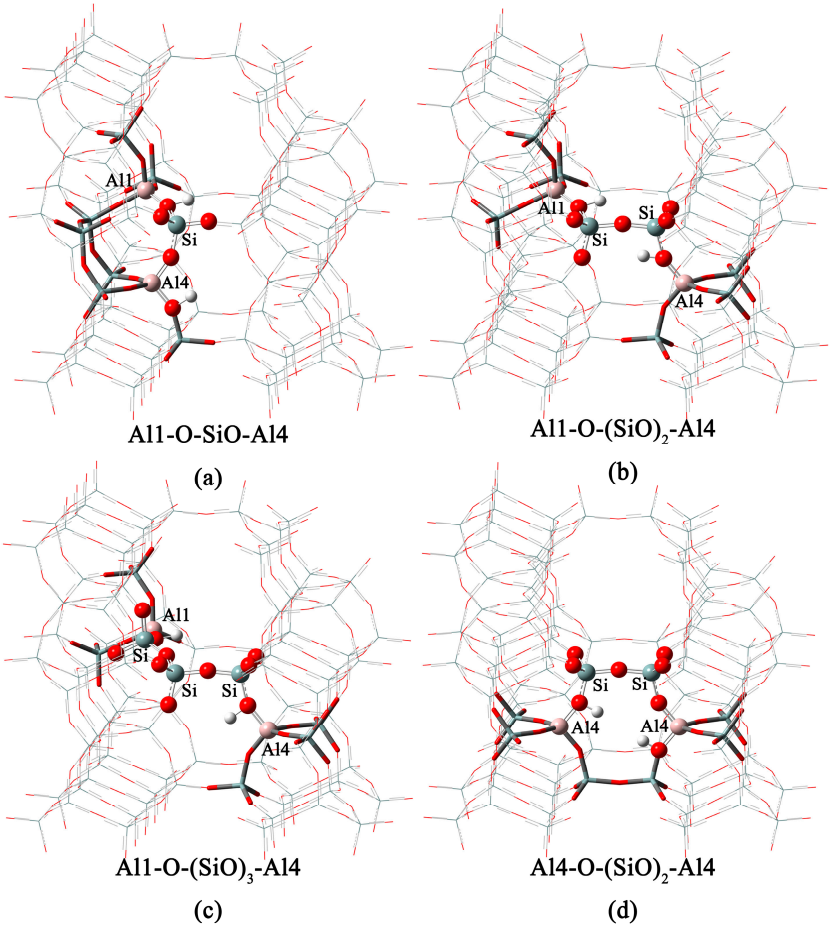

Figure 2. Four different geometrically optimized structures, which have a different number of SiO between Al atoms in 2-Al substitution models, are displayed. T1 and T4 sites are substituted in models (**a**), (**b**) and (**c**), and these models have different amounts of SiO groups between Al atoms. When there are two SiO between Al atoms, two T4 sites in the same 6-membered ring are also populated by Al and is shown in model (**d**). On the 90T model, the region depicted by balls and tubes was treated at high-level and the rest was treated at low-level.

The S_E(Si/Al) and E_D for the 2-Al substitution are listed in Table 2. The Al4-O-(SiO)$_2$-Al4 site has the lowest S_E(Si/Al), suggesting the most stable configuration of Brönsted acid formation in the 2-Al substitution models. Herein the Al4-O-(SiO)$_2$-Al4 sequence is located in one 6-membered ring; the experiments carried out by Dedecek and his co-workers [23] identified the locations of the Al-O-(SiO)$_2$-Al in a ring, which is excellently consistent with our result. The Al1-O-(SiO)$_n$-Al4 (n = 2, 3) configurations have a similar S_E(Al/Si) of around 15 kcal/mol, indicating that the stability exhibits little dependency on the number of SiO groups between the two Al sites. Then the locations of acidic protons indeed have a small effect on the stability of the overall Brönsted acid. However, the Al1-O-Si-O-Al4 sequences have the highest S_E(Si/Al), indicating that the most unstable structure consisted of one SiO group between Al1 and Al4. This result was in agreement with Takaishi et al., who reported that Al-O-Si-O-Al pairs were usually not present in zeolites with Si/Al > 8 [32].

According to the above discussion, the presence of the proton in the Al4-O6-Si2 site leads to the formation of an intra-zeolite hydrogen bond and makes the Al4-O6-Si2 site more stable than other sites. In the Al4-O-(SiO)$_2$-Al4 model, two hydrogen bonds pointing to opposite directions are formed. In Figure 3, we show the hydrogen bonds in the 6-membered ring in n-Al (n = 1,2) substitution. The two hydrogen bonds in Al4-O-(SiO)$_2$-Al4 overlap and reinforce each other, leading to the remarkable deformation of the 6-membered ring. This phenomenon is agreement with the previous

study, which has also described the deformation of 6-membered ring in Fe^{2+} substituted FER [33]. In the absence of hydrogen, the average value of ∠Al4-O-Si2 increases from 141.4° to 143.9° with the substitution of the Si atom by the second Al atom. Moreover, the ∠Al4-O-Si2 decreases obviously upon the addition of H atoms. With the number of Al atoms increasing from one to two, the lengths of the hydrogen bonds decrease from 2.52 to 1.99 Å, indicating that the interaction of two hydrogen bonds can increase their strength The detail structure parameters were shown in Table 3.

Table 2. Characterization of stability and acid strength of Brönsted acid sites calculated on *n*-Al models ($n \geq 2$).

Substitution Site		S_E(Al/Si) (kcal/mol)	E_D (kcal/mol)
T1-O(SiO)-T4	Al1-OH-()-OH-Al4	17.1	3.8
	Al1-OH-()-Al4-OH	16.8	3.1
T1-O$(SiO)_2$-T4	Al1-OH-()-OH-Al4	16.6	3.4
	Al1-OH-()-Al4-OH	14.9	5.1
T1-O$(SiO)_3$-T4	Al1-OH-()-OH-Al4	15.1	0
	Al1-OH-()-O-Al4-OH	15.3	5.0
T4-O$(SiO)_2$-T4	Al4-OH-()-Al4-OH	0	7.7
	Al4-OH-()-OH-Al4	7.8	6.5
T1-T4-T4 (Al > 2)	Al1-O1-Si3	1.9	33.6
	Al1-O2-Si2	6.6	28.9
	Al1-O3-Si1	3.6	31.9

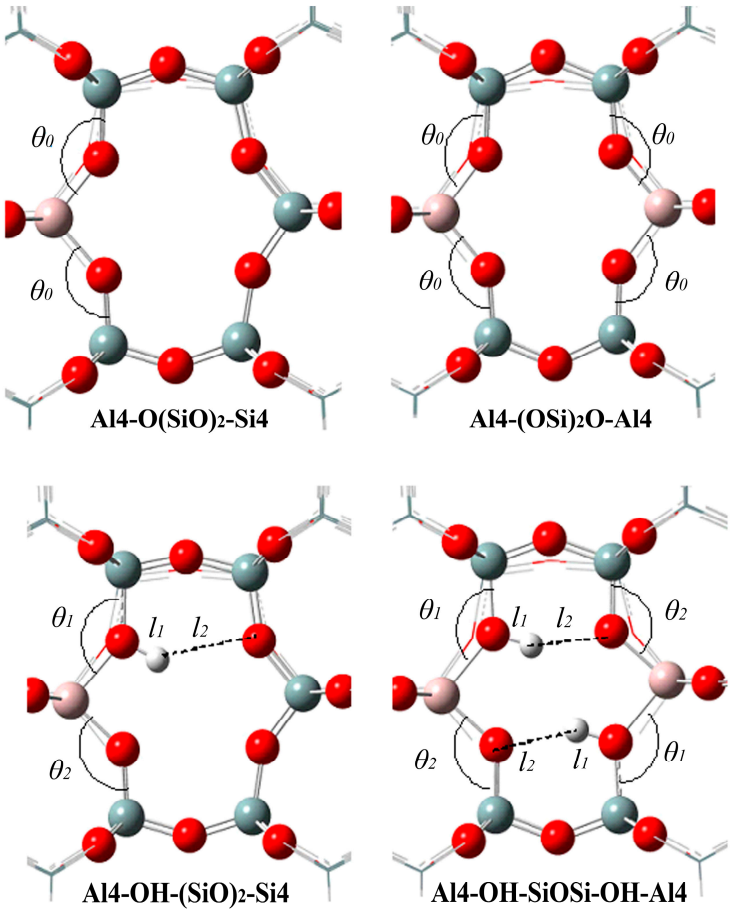

Figure 3. Location of the hydrogen bonds in Al4-O$(SiO)_2$-Si4 and Al4-$(OSi)_2$O-Al4 sites.

Table 3. Structure parameters of T4-O$(SiO)_2$-T4 [1].

Substitution Site	θ_0/(°)	θ_1/(°)	θ_2/(°)	l_1/Å	l_2/Å
Al4-O$(SiO)_2$-Si4	141.4	-	-	-	-
Al4-$(OSi)_2$O-Al4	143.9	-	-	-	-
Al4-OH-$(SiO)_2$-Si4	-	139.1	135.5	0.97	2.52
Al4-OH-SiOSi-OH-Al4	-	136.3	130.3	0.98	1.99

[1] These parameters are averages. θ_0, θ_1 and θ_2 are shown in Figure 3.

The deprotonating energies E_D in 2-Al substituted models are shown in Table 2. For the Al1-O$(SiO)_n$-Al4 (n = 1,2,3) site, it is found that the E_D values follow the order Al1-O(SiO)-Al4 < Al1-O$(SiO)_2$-Al4 < Al1-O$(SiO)_3$-Al4, indicating that the Brönsted acid strengths increase as the number of SiO groups between Al atoms increase. This result is similar to the result of the study of the double acid strength of the H-MCM-22 zeolite by Zhou et al. [17]. As a result, Al1-O$(SiO)_3$-Al4 turns out to be the strongest acid site. Moreover we find that the location of hydrogen protons can also affect the acid strength of Brönsted acid sites. For example, the E_D of the Al-OH-Si-Al-OH site is lower than that of the Al-OH-Si-OH-Al site; a similar trend is found for the Al-OH-(SiOSi)-OH-Al site and the Al-OH-(SiOSi)-Al-OH site. These imply that the 2-Al substitution configuration with two protons located between Al atoms exhibits stronger acidity than that with only one proton located between Al atoms. In addition, the Al4-OH-()-Al4-OH site exhibits the lowest acidity, suggesting that the presence of hydrogen bonds causes the acid strength to decrease.

Based on above analysis, Al4-O6-Si2 and Al4-O-$(SiO)_2$-Al4 is the most stable configuration for 1-Al substitution and 2-Al substitution. We thus speculate that the T4 site is most preferred site for Al substitution. Assuming that the content of Al is very high, all T4 sites would be populated by Al atoms and T1 would be the substitution site for the rest of Al. According to Loewenstein's rule (Al-O-Al sequences are not allowed to occur in any zeolite frameworks), we test three possible sites around the T1 site for the proton location (Figure 4). The E_D of Al1-O1-Si3, Al1-O2-Si2, and Al1-O3-Si1 is listed in Table 2. It is found that, in this case, the Al1-O1-Si3 site is the most stable site, while the Al1-O2-Si2 site is the most unstable site with the strongest acidity. The E_D of n-Al (n > 2) substitution models is the much higher compared with the 2-Al substitution models, indicating that the Brönsted acid strength trends to decline with the substitution of an increasing number of Al atoms. These results agree with the previous experimental study by Zhao et al. [34]. We note that in the present study we only considered an ideal model for Al substitution and may not reproduce the realistic condition where the distribution of Brönsted acid sites could be affected by many other factors [4,14].

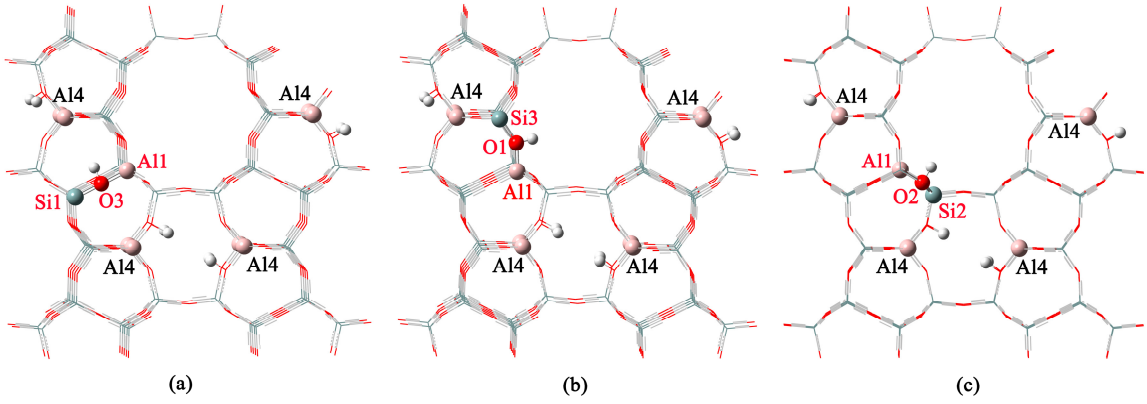

Figure 4. The distribution of Al atoms if the content of Al is so high that all T4 sites are substituted by Al atoms.

2.3. Butene Activation

After considering the stability and acid strength for different Al substitution sites, we now discuss the effect of these properties on the activity of double-bond isomerization of 1-butene to 2-butene. The most stable sites (Al4-O6-Si2 and Al4-O-$(SiO)_2$-Al4) and the strongest acid sites (Al3-O7-Si4 and Al1-O-$(SiO)_3$-Al4) in 1-Al substitution and 2-Al substitution are considered reactive sites. Although two reaction mechanisms of the double bond isomerization, namely stepwise and concerted pathways, have been proposed, it is generally accepted by both experimental and theoretical studies that the concerted mechanism, without the formation of either carbenium ions or covalent alkoxy intermediates, is preferred on zeolite [35,36]. Therefore, in the present study, we only consider the concerted mechanism for the isomerization of 1-butene, and our main aim is to elucidate how the stability and acid strength affect the isomerization reactivity.

The optimized configurations on these four sites are presented in Figure 5. First 1-butene adsorbs on the Brönsted acid site via a π-complex, consistent with the experimental result [37]. The calculated C=C bond lengths of adsorbed 1-butene are all around 1.34 Å, which are close to that of the isolated 1-butene (1.33 Å), suggesting the physical adsorption of 1-butene on these sites. Next the proton (H1) at the Brönsted acid site interacts with C1, and, simultaneously, one hydrogen (H2) in the methylene group attacks the lattice oxygen of the zeolite, achieving the conversion of the C1=C2 double bond into a C2=C3 double bond. This leads to the formation of 2-butene, which also adsorbs on the zeolite via a π-complex. Finally the 2-butene is released into the gas phase, completing the catalytic cycle. The energy profiles on these four different active sites are shown in Figure 6. For 1-Al substitution, the barrier of the isomerization on the strongest acid site, Al3-O7-Si4, is 21.8 kcal/mol, lower than that on the most stable site, Al4-O6-Si2 (25.1 kcal/mol). The same trend is observed in 2-Al substitution cases. The strongest acid site, Al1-O-$(SiO)_3$-Al4, has a low barrier of 18.1 kcal/mol, while the stable Al4-O-$(SiO)_2$-Al4 site (weak acid site) has a high barrier of 27.6 kcal/mol. It is concluded that the strength of the Brönsted acid site directly controls the reactivity for the isomerization of 1-butene to 2-buteneand the stability of acid sites have little influence on reactivity. In addition, although the reaction mechanisms at other site should be similar, the energetics should be different. As the energetics for both the most stable and the least stable sites are presented, it is reasonable to infer that the energetics at other sites should be in between these values.

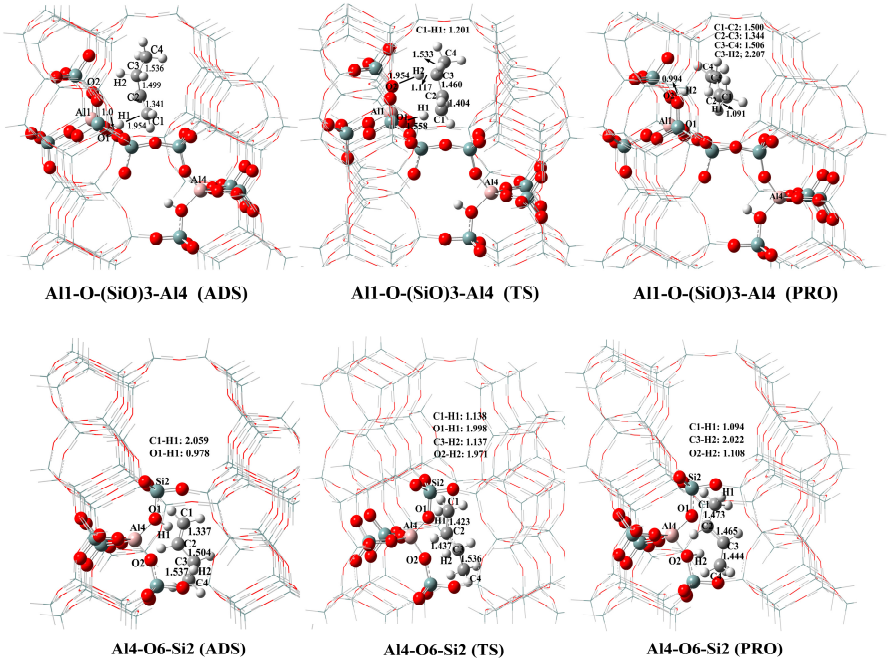

Figure 5. *Cont.*

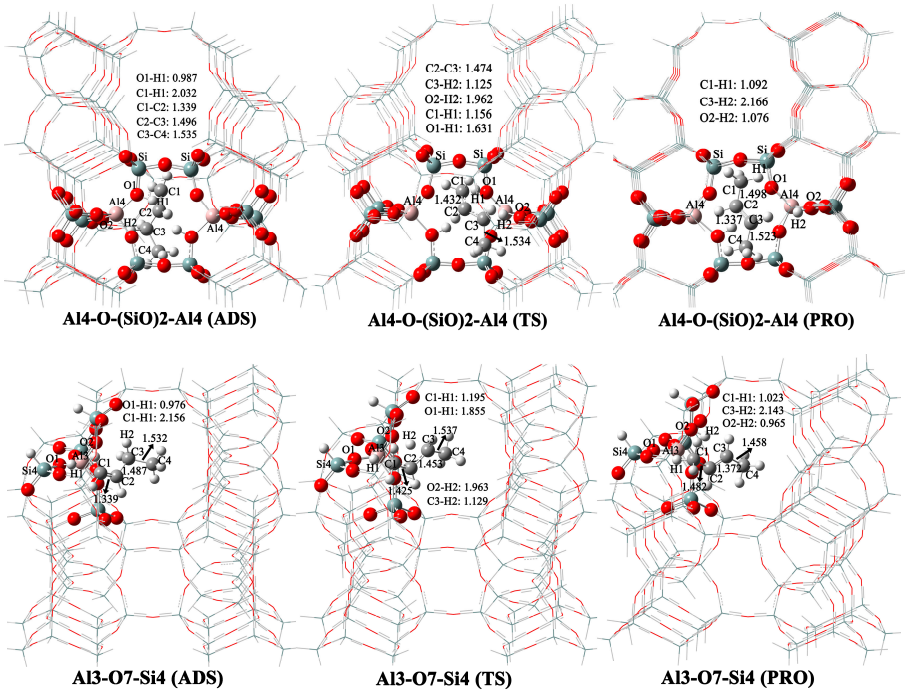

Figure 5. The optimized structures and the values of the most important geometric parameters on four active sites.

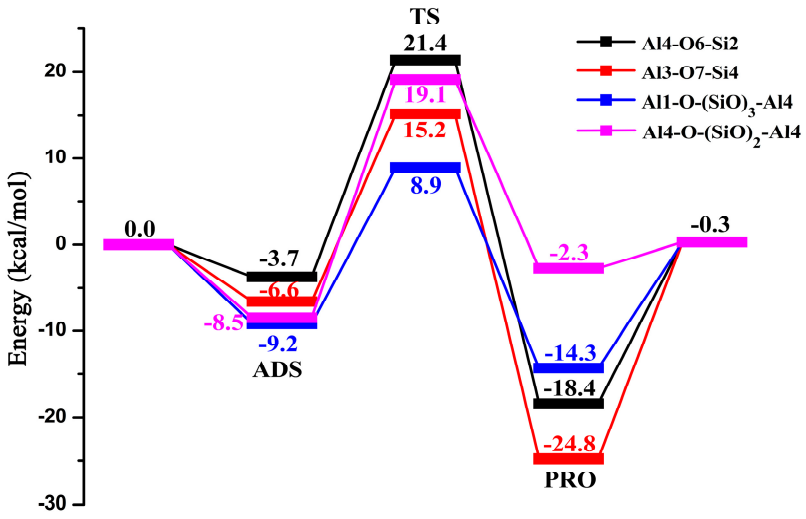

Figure 6. The energy profiles of the isomerization of 1-butene to 2-butene over the different Brönsted acid sites.

3. Computational Details

FER has an orthorhombic unit cell (UC) with the Immm space group. Four tetrahedral sites and eight symmetrically independent framework-oxygen atoms are present in this space group [38]. The 10-membered ring channels that are parallel to the [001] crystallographic direction and 8-membered ring channels that are parallel to the [010] direction intersect each other in FER. A FER unit cell has four un-equivalent T sites that can be occupied by either an Al atom or a Si atom. One T-site is occupied with the Al atom and can form 12 equivalent Brönsted acid sites in FER zeolite. In the present study, a 90T cluster model, including a complete 10-membered ring and a complete 8-membered ring of the bi-dimensional channel system (see Figure 7), was built. We considered the distribution of n-Al sites ($n \geq 1$), which replace the Si sites in the FER zeolite framework. Then the reaction mechanism for

the double-bond isomerization of 1-butene to 2-butene at various Brönsted acid sites were studied to investigate the catalytic properties of FER zeolite.

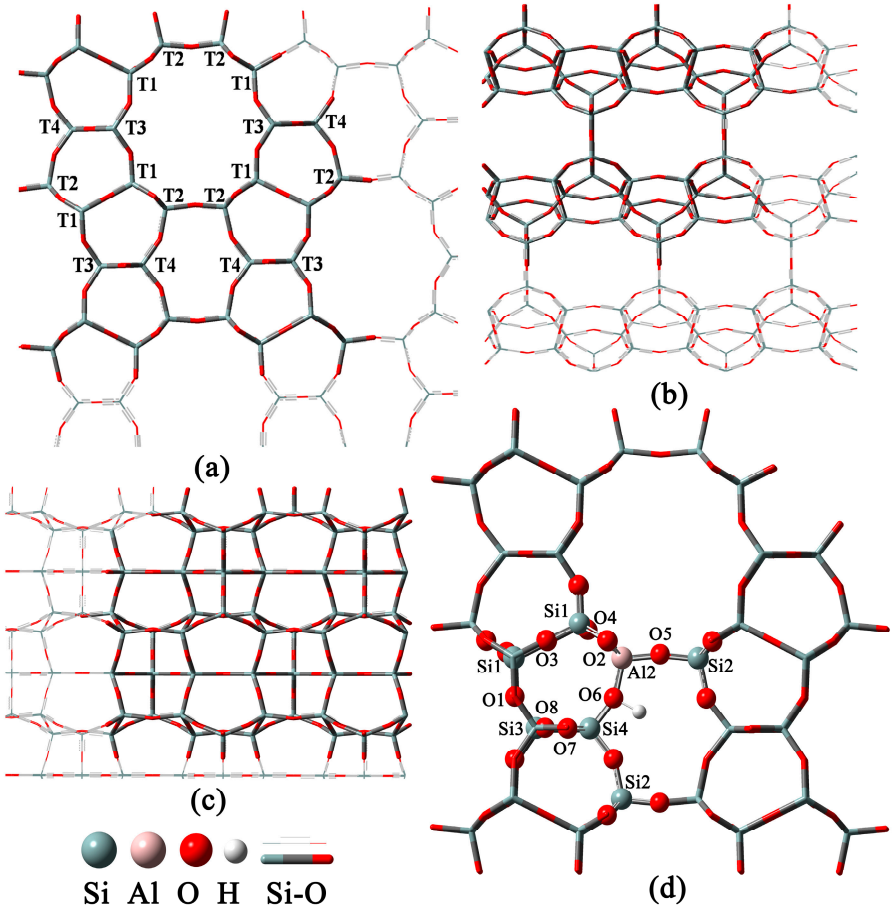

Figure 7. The structure of FER zeolite. (**a**) is the projection along [001], (**b**) [010], and (**c**) [100]. 90T is cut out from cluster (**a**) as the model in this study. Locations of all T sites are shown in (**a**). T1, T2s and T3 are located on the 10-membered ring; T1, T2, and T4 are on the surface of the FER cage. 1-Al substitution models are shown in (**d**). When the T2 site was studied, the region (10T), depicted by balls around the center T2 site, was treated at high-level and the rest was treated at low-level.

All calculations were carried out by the Gaussian 09 package (Revision C.01; Gaussian, Inc.: Wallingford, CT, USA, 2010) [39]. The two-layer ONIOM methodologies [40] combined with the quantum mechanics/molecular mechanics (QM/MM) calculations were applied in this study, which has proved to be efficient in investigating many reaction mechanisms in zeolite pore networks [10,41]. The region in an intimate relationship to catalytic reactions is treated at a high level with the B3LYP/6-31G (d, p) method for accuracy [36], while regions away from the active center are treated at a lower level with the semi-empirical calculation method for efficiency. In Figure 7d, a 10T region surrounding the substituted T sites, depicted by balls in the models, was treated as high-level and all atoms in this region were relaxed in order to be optimized. The rest was described by the low-level semi-empirical method and all the atoms in this region were fixed to retain the structure. The dangling bonds connecting the 90T clusters with the rest of the zeolite were saturated with hydrogen atoms. The dangling bonds that were oriented towards the positions were occupied by the oxygen atoms in the next coordination sphere, and the distance between hydrogen atoms and the Si atoms was 1.47 Å. Moreover all charges were compensated by hydrogen ions. For the investigation of the double-bond isomerization of 1-butene to 2-butene at various Brönsted acid sites, 1-butene and 2-butene were also treated at a high level. All minima (no imaginary frequencies) and

transition states (one imaginary frequency) were characterized by calculating the Hessian matrix. The optimization of transition state was calculated using the synchronous quasi-Newtonian method (QST3) [42]. The identity of the transition states was confirmed by following the intrinsic reaction coordinates (IRC).

To explore the distribution of Brönsted acid sites, we considered the thermodynamic stability by calculating the substitution energy, which is calculated by finding the difference between the related energy for the pure siliceous structure and that for the corresponding Al-substituted cluster model;

$$S_E(\mathrm{Al/Si}) = E(\text{Al-OH-Si}) - E(\text{Si-O-Si}) \quad (1)$$

The lower $S_E(\mathrm{Al/Si})$ associates with a more stabilized, corresponding, Al-substituted structure. The most stable configuration is considered the energy reference state in each n-Al model. The deprotonation energy E_D was employed to characterize the acid strengths of Brönsted acid sites. It is calculated according to the formula;

$$E_D = E(\text{Zeo-OH}) - E(\text{Zeo-O}^-) \quad (2)$$

where E(Zeo-OH) represents the energy of a system with a Brönsted acid site and E(Zeo-O^-)represents the energy of the same system, with the H^+ being removed. The deprotonation energy is usually used to evaluate the difficulty of ionizing hydrogen. Therefore a Brönsted acid site with stronger acidity usually has a lower E_D. The system with the lowest E_D in each n-Al model is considered the energy reference state.

4. Conclusions

The $S_E(\mathrm{Si/Al})$ and E_D were used to characterize the distribution and strength of Brönsted acid sites in n-Al ($n \geq 1$) substituted models by DFT calculations. Based on the results of the Al distribution in 1-Al substitution models, Al4-O-$(SiO)_2$-Al4 and Al1-O-$(SiO)_n$-Al4 (n = 1,2 or 3) were considered to be the possible locations in 2-Al substitution models. The calculation results showed that the hydrogen bond could improve the stability of Bronsted acid sites effectively. As a result, Al4-O6-Si2 and Al4-O-$(SiO)_2$-Al4 are the most stable sites for 1-Al substitution and 2-Al substitution, respectively. According to the results of E_D, the Brönsted acid strength tends to decrease with the increase of Al contents and increase when the distance between the Al atoms is increased in 2-Al substitution. However, the distance between the two Al atoms has little influence on the distribution of the Brönsted acid sites in 2-Al substitution models. In addition, though the present study was considered an ideal model for Al substitution, the trend also revealed that the distribution of Al in a FER molecular sieve was not random. The properties of the acid sites have a significant influence on the reaction. Therefore the catalytic activity for the double bond isomerization of 1-butene to 2-butene on different active sites was also discussed, and it was revealed that the strength of acid sites determined the reactivity.

Acknowledgments: The authors are grateful for the financial support of the National Natural Science Foundation of China (Projects 20126008).

Author Contributions: Biaohua Chen and Jie Zhang conceived and designed the experiments; Miao He and Rui Liu performed the experiments; Miao He and Xiuliang Sun analyzed the data; Xiuliang Sun contributed analysis tools; Miao He wrote the paper.

Conflicts of Interest: The authors declare no conflict of interest.

References

1. Pavlov, M.L.; Shavaleev, D.A.; Kutepov, B.I.; Travkina, O.S.; Pavlova, I.N.; Basimova, R.A.; Ershtein, A.S.; Gerzeliev, I.M. Synthesis and investigation of ZSM-5 zeolite-based catalysts for benzene alkylation with ethylene. *Petrol. Chem.* **2016**, *56*, 151–157. [CrossRef]

2. Jin, W.K.; Kim, D.J.; Han, J.U.; Min, K.; Ji, M.K.; Yie, J.E. Preparation and characterization of zeolite catalysts for etherification reaction. *Catal. Today* **2003**, *87*, 195–203.
3. Khitev, Y.P.; Ivanova, I.I.; Kolyagin, Y.G.; Ponomareva, O.A. Skeletal isomerization of 1-butene over micro/mesoporous materials based on FER zeolite. *Appl. Catal. A* **2012**, *441–442*, 124–135. [CrossRef]
4. Sklenak, S.; Li, C.; Wichterlová, B.; Gábová, V.; Sierka, M.; Sauer, J. Aluminum siting in silicon-rich zeolite frameworks: A combined high-resolution ^{27}Al NMR spectroscopy and quantum mechanics / molecular mechanics study of ZSM-5. *Angew. Chem. Int. Ed.* **2007**, *46*, 7286–7289. [CrossRef] [PubMed]
5. Bokhoven, J.A.V.; Lee, T.L.; Drakopoulos, M.; Lamberti, C.; Thiess, S.; Zegenhagen, J. Determining the aluminium occupancy on the active T sites in zeolites using X-ray standing waves. *Nat. Mater.* **2008**, *7*, 551–555. [CrossRef] [PubMed]
6. Houžvička, J.; Ponec, V. Skeletal isomerisation of *N*-butene on phosphorus containing catalysts. *Appl. Catal. A* **1996**, *145*, 95–109. [CrossRef]
7. Maciver, D.S.; Wilmot, W.H.; Bridges, J.M. Catalytic aluminas: II. Catalytic properties of eta and gamma alumina. *J. Catal.* **1964**, *3*, 502–511. [CrossRef]
8. Donk, S.V.; Bus, E.; Broersma, A.; Bitter, J.H.; Jong, K.P.D. Probing the accessible sites for *n*-butene skeletal isomerization over aged and selective H-ferrierite with *d*3-acetonitrile. *J. Catal.* **2002**, *212*, 86–93. [CrossRef]
9. Hu, Y.; Liu, L.; Zhang, H.; Hu, L.; Zhang, C.; Zhang, H. Effect of crystal size on the skeletal isomerization of *n*-butene over H-FER zeolite. *React. Kinet. Mech. Cat.* **2014**, *112*, 241–248. [CrossRef]
10. Gleeson, D. Skeletal isomerization of butene in ferrierite: Assessing the energetic and structural differences between carbenium and alkoxide based pathways. *J. Phys. Chem. A* **2011**, *115*, 14629–14636. [CrossRef] [PubMed]
11. Oyoung, C.L.; Pellet, R.J.; Casey, D.G.; Ugolini, J.R.; Sawicki, R.A. Skeletal isomerization of 1-butene on 10-member ring zeolite catalysts. *J. Catal.* **1995**, *151*, 467–469. [CrossRef]
12. Dědeček, J.; Kaucký, D.; Wichterlová, B.; Gonsiorová, O. Co^{2+} ions as probes of Al distribution in the framework of zeolites ZSM-5 study. *Phys. Chem. Chem. Phys.* **2002**, *4*, 5406–5413. [CrossRef]
13. Dědeček, J.; Kaucký, D.; Wichterlová, B. Al distribution in ZSM-5 zeolites: An experimental study. *Chem. Commun.* **2001**, *11*, 970–971. [CrossRef]
14. Sklenak, S.; Dedecek, J.; Li, C.; Wichterlová, B.; Gábová, V.; Sierka, M.; Sauer, J. Aluminium siting in the ZSM-5 framework by combination of high resolution ^{27}Al NMR and DFT/MM calculations. *Phys. Chem. Chem. Phys.* **2009**, *11*, 1237–1247. [CrossRef] [PubMed]
15. Sklenak, S.; Andrikopoulos, P.C.; Whittleton, S.R.; Jirglova, H.; Sazama, P.; Benco, L.; Bucko, T.; Hafner, J.; Sobalik, Z. Effect of the Al siting on the structure of Co(II) and Cu(II) cationic sites in ferrierite. A periodic DFT molecular dynamics and FTIR Study. *J. Phys. Chem. C* **2013**, *117*, 3958–3968. [CrossRef]
16. Sastre, G.; Katada, N.; Suzuki, K.; Niwa, M. Computational study of Brønsted acidity of Faujasite: Effect of the Al content on the infrared OH stretching frequencies. *J. Phys. Chem. C* **2008**, *63*, 19293–19301. [CrossRef]
17. Zhou, D.; Ying, B.; Yang, M.; Ning, H.; Gang, Y. DFT studies on the location and acid strength of Brönsted acid sites in MCM-22 zeolite. *J. Mol. Catal. A* **2006**, *244*, 11–19. [CrossRef]
18. Lo, C.; Trout, B.L. Density functional theory characterization of acid sites in chabazite. *J. Catal.* **2004**, *227*, 77–89. [CrossRef]
19. Dědeček, J.; Sklenak, S.; Li, C.; Wichterlová, B.; Gábová, V.; Brus, J.; Sierka, M.; Sauer, J. Effect of Al−Si−Al and Al−Si−Si−Al pairs in the ZSM-5 zeolite framework on the ^{27}Al NMRspectra. A combined high-resolution ^{27}Al NMR and DFT/MM study. *J. Phys. Chem. C* **2009**, *113*, 1447–1458. [CrossRef]
20. Sazama, P.; Tabor, E.; Klein, P.; Wichterlova, B.; Sklenak, S.; Mokrzycki, L.; Pashkkova, V.; Ogura, M.; Dedecek, J. Al-rich beta zeolites distribution of Al atoms in the framework and related protonic and metal-ion species. *J. Catal.* **2016**, *333*, 102–114. [CrossRef]
21. Mooiweer, H.H.; Jong, K.P.D.; Kraushaar-Czametzki, B.; Stork, W.H.J.; Krutzen, B.C.H. Skeletal isomerization of olefins with the zeolite ferrierite as catalyst. *Stud. Surf. Sci. Catal.* **1994**, *84*, 2327–2334.
22. Houžvička, J.; Hansildaar, S.; Ponec, V. The shape selectivity in the skeletal isomerization of *n*-butene to isobutene. *J. Catal.* **1997**, *167*, 273–278. [CrossRef]
23. Dedecek, J.; Lucero, M.J.; Li, C.; Gao, F.; Klein, P.; Urbanova, M.; Tvaruzkova, Z.; Sazama, P.; Sklenak, S. Complex analysis of the aluminum siting in the framework of silicon-rich zeolites. A case study on ferrierites. *J. Phys. Chem. C* **2011**, *115*, 11056–11064. [CrossRef]

24. Simperler, A.; Bell, R.; Anderson, M. Probing the acid strength of Brönsted acidic zeolites with acetonitrile: Quantum chemical calculation of H1, N15 and C^{13} NMR shift parameters. *J. Phys. Chem. B* **2004**, *108*, 7142–7151. [CrossRef]
25. Liu, R.; Zhang, J.; Sun, X.; Huang, C.; Chen, B. An oniom study on the distribution, local structure and strength of Brönsted acid sites in FER zeolite. *Comput. Theor. Chem.* **2014**, *1027*, 5–10. [CrossRef]
26. Benco, L.; Bucko, T.; Grybos, R.; Hafner, J.; Sobalik, Z.; Dedecek, J.; Hrusak, J. Adsorption of NO in Fe^{2+}-exchanged ferrierite. A density functional theory study. *J. Phys. Chem. C* **2007**, *111*, 586–595. [CrossRef]
27. Kikhtyanin, O.; Kubička, D.; Čejkab, J. Toward understanding of the role of Lewis acidity in aldol condensation of acetone and furfural using MOF and zeolite catalysts. *Catal. Today* **2015**, *243*, 158–162. [CrossRef]
28. Grajciar, L.; Arean, C.O.; Pulido, A.; Nachtigall, P. Periodic DFT investigation of the effect of aluminium content on the properties of the acid zeolite H-FER. *Phys. Chem. Chem. Phys.* **2010**, *12*, 1497–1506. [CrossRef] [PubMed]
29. Feng, P.; Chen, X.F.; Li, X.J.; Zhao, D.; Xie, S.J.; Xu, L.Y.; He, G.Z. The distribution analysis on the proton siting and the acid strength of the zeolite ferrierite: A computational study. *Microporous Mesoporous Mater.* **2017**, *239*, 354–362. [CrossRef]
30. Nachtiqall, P.; Bludsky, O.; Grajciar, L.; Nachtiqallova, D.; Delgado, M.R.; Arean, C.O. Computational and FTIR spectroscopic studies on carbon monoxide and dinitrogen adsorption on a high-silica H-FER zeolite. *Phys. Chem. Chem. Phys.* **2009**, *11*, 791–802. [CrossRef] [PubMed]
31. Simperler, A.; Bell, R.G.; Foster, M.D.; Gray, A.E.; Lewis, D.W.; Anderson, M.W. Probing the acid strength of Brönsted acidic zeolites with acetonitrile: An atomistic and quantum chemical study. *J. Phys. Chem. B* **2004**, *108*, 7152–7161. [CrossRef]
32. Takaishi, T.; Kato, M.; Itabashi, K. Stability of the Al-O-Si-O-Al linkage in a zeolitic framework. *J. Phys. Chem.* **2002**, *98*, 5742–5743. [CrossRef]
33. Benco, L.; Bucko, T.; Hafner, J. Activity and reactivity of Fe^{2+} cations in the zeolite: Ab initio free-energy MD calculation of the N_2O dissociation over iron-exchanged ferrierite. *J. Phys. Chem. C* **2009**, *113*, 18807–18816. [CrossRef]
34. Zhao, G.; Teng, J.; Zhang, Y.; Xie, Z.; Yue, Y.; Chen, Q.; Yi, T. Synthesis of ZSM-48 zeolites and their catalytic performance in C4-olefin cracking reactions. *Appl. Catal. A* **2006**, *299*, 167–174. [CrossRef]
35. Boronat, M.; Viruela, P.; Corma, A. Theoretical study of the mechanism of zeolite-catalyzed isomerization reactions of linear butenes. *J. Phys. Chem. A* **1998**, *102*, 982–989. [CrossRef]
36. Li, H.Y.; Pu, M.; Liu, K.H.; Zhang, B.F.; Chen, B.H. A density functional theory study on double-bond isomerization of 1-butene to *cis*-2-butene catalyzed by zeolites. *Chem. Phys. Lett.* **2005**, *404*, 384–388. [CrossRef]
37. Kondo, J.N.; Domen, K. IR observation of adsorption and reactions of olefins on H-form zeolites. *J. Mol. Catal. A* **2003**, *199*, 27–38. [CrossRef]
38. Vaughan, P.A. The crystal structure of the zeolite ferrierite. *Acta Crystallogr.* **1966**, *21*, 983–990. [CrossRef]
39. Frisch, M.J.; Trucks, G.W.; Schlegel, H.B.; Scuseria, G.E.; Robb, M.A.; Cheeseman, J.R.; Scalmani, G.; Barone, V.; Mennucci, B.; Petersson, G.A.; et al. *Gaussian 09*, Revision C.01; Gaussian, Inc.: Wallingford, CT, USA, 2010.
40. Wattanakit, C.; Nokbin, S.; Boekfa, B.; Pantu, P.; Limtrakul, J. Skeletal isomerization of 1-butene over ferrierite zeolite: A quantum chemical analysis of structures and reaction mechanisms. *J. Phys. Chem. C* **2012**, *116*, 5654–5663. [CrossRef]
41. Ferrante, F.; Rubino, T.; Duca, D. Butene isomerization and double-bond migration on the H-ZSM-5 outer surface: A density functional theory study. *J. Phys. Chem. C* **2011**, *115*, 14862–14868. [CrossRef]
42. Fellah, M.F.; Santen, R.A.V.; Onal, I. Oxidation of benzene to phenol by N_2O on an Fe^{2+}-ZSM-5 cluster: A density functional theory study. *J. Phys. Chem. C* **2009**, *113*, 15307–15313. [CrossRef]